https://doi.org/10.1007/s11467-022-1184-z

RESEARCH ARTICLE

High efficiency giant magnetoresistive device based on two-dimensional MXene (Mn_2NO_2)

Xiaolin Zhang[1], Pengwei Gong[1], Fangqi Liu[1], Kailun Yao[2], Jian Wu[3], Sicong Zhu[1,†]

[1] The State Key Laboratory for Refractories and Metallurgy, Hubei Province Key Laboratory of Systems Science in Metallurgical Process, Collaborative Innovation Center for Advanced Steels, International Research Institute for Steel Technology, Wuhan University of Science and Technology, Wuhan 430081, China

[2] Wuhan National High Magnetic Field Center and School of Physics, Huazhong University of Science and Technology, Wuhan 430074, China

[3] College of Advanced Interdisciplinary Studies, National University of Defense Technology, Changsha 410073, China

Corresponding author. E-mail: [†]sczhu@wust.edu.cn

Received February 23, 2022; accepted June 3, 2022

Supporting Information

Table S1 shows the distances before optimization, system energy of Mn_2NO_2/Au, and optimized bond lengths of Au and O atoms in the device construction stage. The optimized bond lengths are all around 2.3 Å after sufficient relaxation implying that a bond length of 2.3 Å for Au-O is more stable and suitable.

Table S1 Placement distance before optimization, system energy of Au and Mn_2NO_2, bond length after optimization.

Distance before optimization (Å)	$E_{Au\text{-}Mn_2NO_2\text{-}Au}$ (eV)	Optimized bond length(Å)
2.2	-17888.11	2.295
2.3	-17887.84	2.270
2.4	-17887.92	2.285
2.5	-17887.97	2.308
2.6	-17888.01	2.315
2.7	-17888.26	2.342

To check the correctness of the calculation with ATK software, we calculated the electronic properties of the structure with VASP software to ensure the accuracy of the model. The 1.8 eV

band gap of the minority-spin of Mn_2NO_2 is somewhat different from that calculated by ATK software. The calculated results show that Mn_2NO_2 is half-metallic.

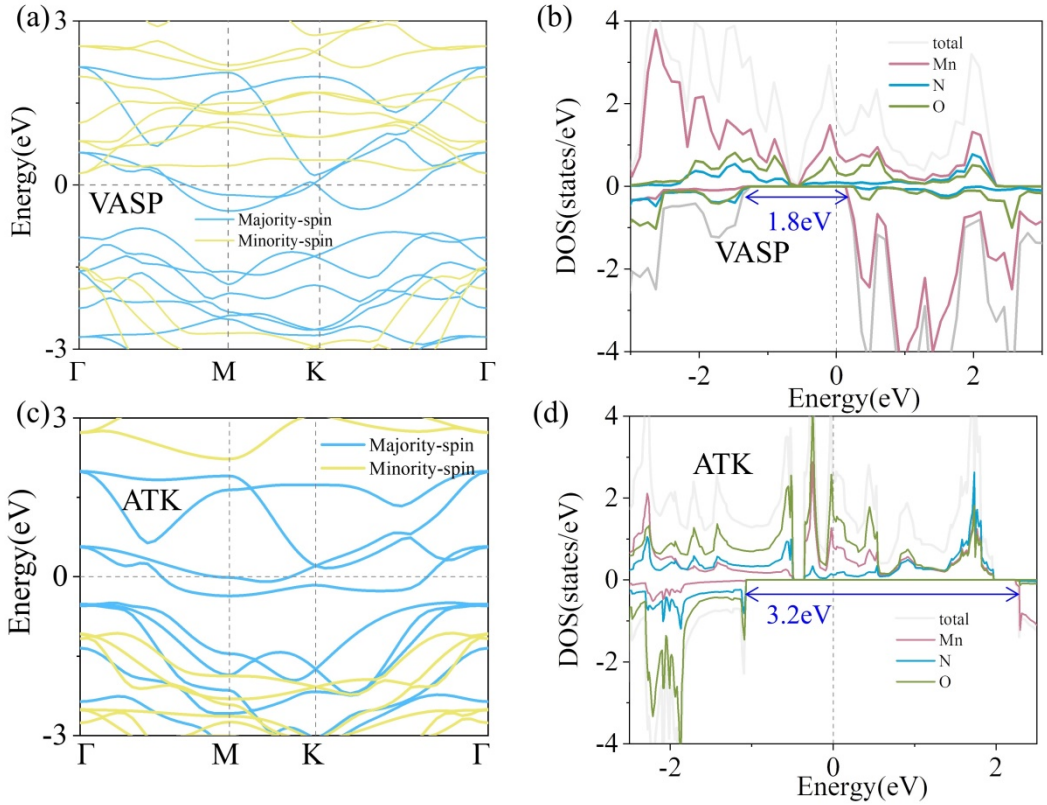

Fig. S1 (a) Band structure for Mn_2NO_2 MXene. **(b)** The DOS of Mn_2NO_2 MXene.The Fermi level in (a) and (b) is set to zero.

In addition, the thermoelectric conversion efficiency of material depends mainly on the euphoria coefficient Z, which is closely related to the thermal property parameters (Seebeck coefficient, electrical conductivity, thermal conductivity) of the thermoelectric material, and the dimensionless euphoria coefficient ZT is usually used as an evaluation index for the performance of thermoelectric materials. We also calculate the thermal conductivity, conductivity, thermoelectric merit, and Seebeck coefficient of Mn_2NO_2 at different temperatures with Nanodcal software (Fig. S2).

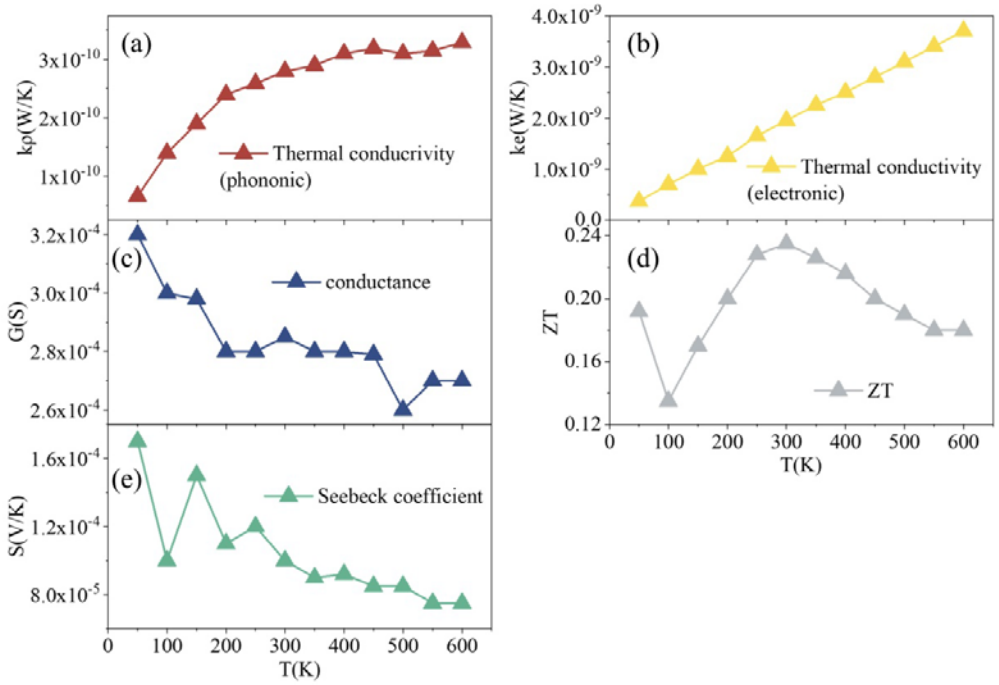

Fig. S2 (a) The phononic thermal conductivity, **(b)** electronic thermal conductivity, **(c)** conductance, **(d)** thermoelectric merit (ZT) and **(e)** Seebeck coefficient of Mn_2NO_2**.**

In Fig. S3, the position of the O atom corresponds to the Mn atom, showing an adsorption energy of 0.26 eV and a layer spacing of 2.56 Å. The stacking mode of Top-N shows 0.24ev adsorption energy and 0.59 Å. The stacking mode of the O atom corresponding to the O atom shows the longest layer spacing and the smallest adsorption energy. These data show that the stacking mode of Top-O is the most unstable and that of Top-Mn is the most stable. In order to verify the influence of the stability of stacking mode on the device structure, we also construct devices for these two stacking modes (Fig. S3(d)). The results show that the two stacking methods have great structural damage after contacting with the Au (111) surface, indicating that the two structures can not be constructed into stable devices. Therefore, in the subsequent discussion, we only consider the stacking mode of Top-Mn and calculate the transmission properties.

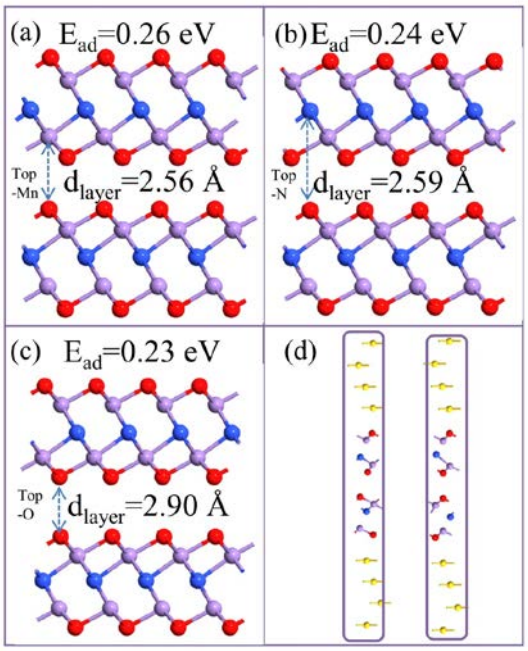

Fig. S3 Three configurations, adsorption energies (E_{AD}), and layer distance (d_{layer}) when O atom is placed on **(a)** top-Mn site, **(b)** top-N site, and **(c)** top-O site. **(d)** metastable structures after relaxation.

The band structure of pure Mn_2NO_2 and interface system is calculated by VASP software. Fig. S4 (a) shows the structure of the interface system shown by VESTA software. The upper and lower layers of Mn_2NO_2 are in contact with the monolayer Au (111) surface respectively. The band structure of the original Mn_2NO_2 without considering spin polarization is compared. For the system after contact, Mn_2NO_2 mainly contributes above the Fermi level.

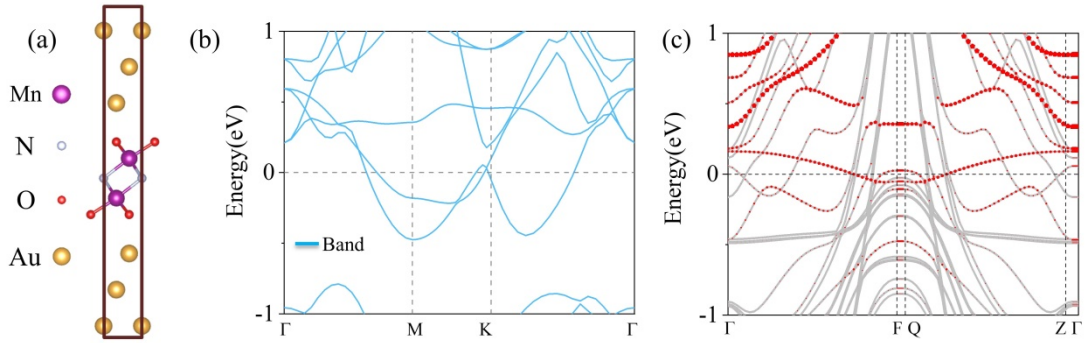

Fig. S4 (a) The structure of the monolayer Mn_2NO_2 in contact with Au (111). **(b)** The band structure of the original Mn_2NO_2 without considering the spin polarization. **(c)** The projected band structure of the contact system of Au/Mn_2NO_2/Au. The red and gray lines indicate Mn_2NO_2 and the total band of the system, respectively.

To describe the interfacial charge distribution, the electron densities of Mn_2NO_2 and Au are plotted in Fig. S5 effective potential (EP) and electron localization function (ELF). The EP of an electron represents its interaction with ionic nuclei and other electrons. The interface tunnel barrier is calculated as the difference between the highest average potential at the contact interface and the highest average potential at the Au (111) surface. The electron density shows the weak binding between Au and Mn_2NO_2. The negative value in Fig. S5 (b) indicates that the structure is ohmic contact, and it can be seen from ELF that there are metal bonds at the interface.

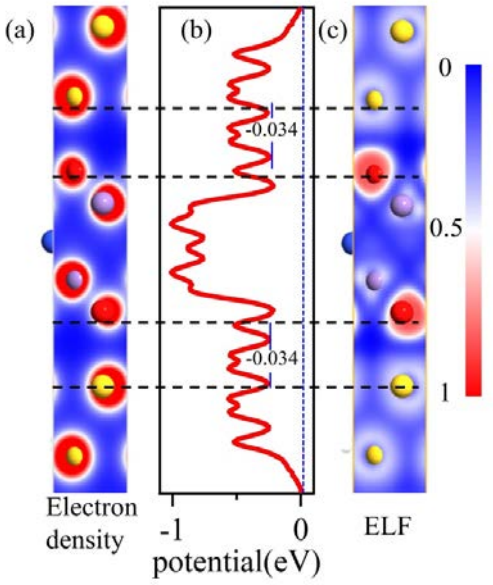

Fig. S5 (a) Electron density of the Au/Mn_2NO_2/Au contact system. **(b)** Effective potential, also shows the average potential barrier at the Mn_2NO_2 and Au interface. **(c)** Contour plot of the ELF.